AFM Analysis of Micron and Sub-micron sized Bridges Fabricated Using the Femtosecond Laser on YBCO Thin Films.

Patrice Umenne [1]

Abstract The project arose as a result of the need to use the femtosecond laser to fabricate sub-micron and Nano-sized bridges that could be analyzed for the Josephson effect. The femtosecond laser has a low pulse duration of 130 femtoseconds. Hence in an optical setup it was assumed that it could prevent the thermal degradation of the superconductive material during fabrication. In this paper a series of micron and sub-micron sized bridges where fabricated on superconductive YBCO thin film using the femtosecond laser, a spherical convex lens of focal length 30 mm and the G-code control programming language applied on a translation stage. The dimensions of the bridges fabricated where analyzed using the Atomic Force Microscope (AFM). As a result, micron sized superconductive bridges of width 1.68 μm, 1.39 μm, 1.23 μm and a sub-micron sized bridge of width 732 nm where fabricated. The length of this bridges ranged from 9.6 μm to 12.8 μm. The femtosecond laser technique and the spherical convex lens can be used to fabricate bridges in the sub-micron dimension.

Keywords: Atomic Force Microscope (AFM); Laser ablation diameter; Separation distance (S_W); Sub-micron bridges; YBCO thin film.

1. Introduction

The main aim of this work was to fabricate sub-micron and Nano sized bridges using the 775 nm wavelength femtosecond laser [1-4] on superconductive YBCO thin film [5-8]. The resulting bridges could then be tested for the presence of the Josephson effect and used as Josephson Junctions [9-13]. The smaller in size the bridges that are fabricated the more likely they are to show the Josephson effect. If proven to show the Josephson effect, they can then be used in applications such as Superconducting Quantum Interference Device (SQUID) [14] to detect the presence of magnetic moments. This papers focus is however restricted to several superconductive bridges fabricated in the achievable micron and sub-micron scale and their dimensional analysis using the Atomic Force Microscope (AFM).

A series of bridges where fabricated utilizing optical equipment such as reflective mirrors, iris diaphragm, spherical convex lens and optical techniques such as beam collimation and beam focusing to a reduce the laser ablation diameter. Optimization techniques where applied such as reducing the laser ablation diameter by lowering the pulse energy of the laser [15] and reducing the width of the bridge by reducing the separation distance between the laser ablation spots (S_w). G-code (RS-274) computer numerical control (CNC) programming language was used to enable the movement of the translation stage that held the thin film sample. In the meantime, the laser was held in a stationary position while ablating the sample. In order to measure the dimensions of the bridges after fabrication the AFM [16-20] was utilized for imaging the sample. The AFM scans where done with type DT-NCHR diamond cantilever tips in tapping mode.

The main hypothesis in the project was the assumption that the low pulse duration of the femtosecond laser of 130 femtoseconds could reduce thermal degradation of the superconductive YBCO thin film. This is required in the fabrication of Josephson Junctions. However, a null hypothesis was achieved. Experiments showed the pulse duration of the laser on the superconductive YBCO thin film during fabrication is actually a combined average of the feed rate of the translation stage which was set at 20 mm/min or 333 $\mu m s^{-1}$, the frequency of the laser or pulse repetition rate in this case 1 kHz and the pulse duration of the laser which is 130 femtoseconds. As a

[1] Department of Electrical and Mining Engineering, University of South Africa; umennpo@unisa.ac.za

result, the time spent by the laser on the YBCO sample during ablation is in fact much longer than femtoseconds. Hence some thermal degradation occurs.

2. Experimental

The YBCO thin films utilized for the experiment where procured from ceraco ceramic GmbH company. The thin films had the following specifications: 9×9 mm YBCO film, single sided 200 nm thickness, one side polished. The YBCO thin films came on either an $LaAlO_3$ substrate or an MgO substrate. The thin films where the S-type smooth matrix useful for the manufacture of SQUIDS and where placed on a substrate of $10 \times 10 \times 0.5$ mm dimension. The critical temperature of the YBCO thin film used was $T_C = 87\ K$.

The laser beam was focused unto the YBCO sample to machine the bridges by using a spherical convex lens of 30 mm focal length. The femtosecond laser power ranged from (0-1000) mW. The laser was set at 2.1 mW in order to cut just slightly above the ablation threshold of the YBCO thin film and hence make the laser ablation diameter as small as possible. This optimization technique facilitates the fabrication of smaller bridges. The laser power setting of 2.1 mW in combination with the spherical convex lens of focal length 30 mm produced a laser ablation diameter of 15.8 μm.

Figure 1 shows the block diagram of the optical set up used to optimize the laser ablation spot size and to fabricate the bridges with the femtosecond laser. The set up consists of the laser source, the beam collimation set up, reflective mirrors, iris (manually adjustable aperture) and the spherical convex lens of 30 mm focal length.

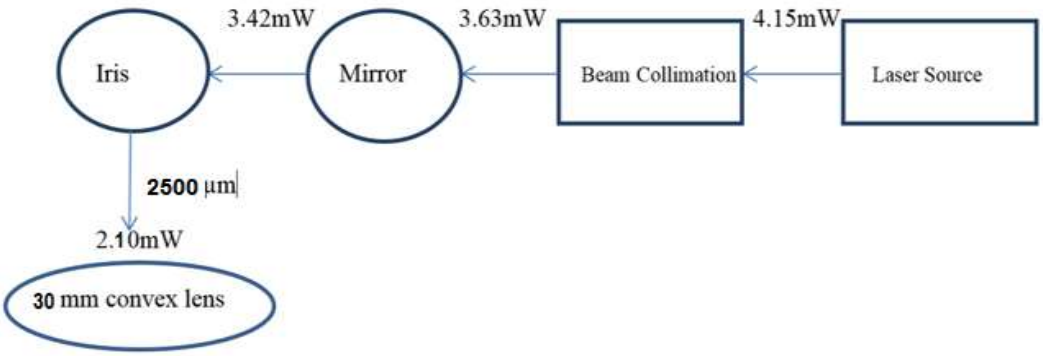

Fig. 1 Block diagram of the overall laser optical experimental set up used to machine the bridges [21].

The function of the iris diaphragm is to remove unwanted sections of the laser in the outer periphery of the laser beam after the beam collimation process. The iris helps remove the poorly shaped sections of the laser beam produced by spherical aberration. This means only the central core of the laser beam would pass through to the focusing optics. The laser beam diameter from the laser source was 9.85 mm. The iris diaphragm could be adjusted from $(0 - 10000)\ \mu m$. The iris was set to a diameter of $2500\ \mu m$, thus reducing the laser beam diameter from 9.85 to $2.5\ mm$. The laser beam is then passed through the focusing optics and a laser ablation diameter of $15.8\ \mu m$ is produced. During fabrication the YBCO sample is placed on a translation stage whose movement is programmed using G-code. The laser was kept stationary while the translation stage moved during the fabrication of the bridges. The width of the bridges after fabrication is defined by the formula in equation (1):

$$width\ of\ bridge = S_W - laser\ ablation\ diameter \quad (1)[21]$$

where S_W is the separation distance between the laser ablation spots along the length of the square sample.

The length of the bridges is defined by the formula in equation (2):

$$Length\ of\ bridge = |S_L - Laser\ ablation\ diameter| \quad (2)$$

where S_L is the separation distance between the laser ablation spots along the width of the square sample.

3. Results and Discussion

Table 1 summarizes the bridges fabricated, the separation distance between the laser ablation diameters S_W set in the program, the laser ablation diameter and the width of the bridge that was machined. During the fabrication of all these bridges a conventional spherical convex lens of focal length 30 mm was used as the focusing optics.

Table 1 Summary of bridges fabricated and their dimensions

Number	Name of bridge	Separation distance between laser ablation spots (S_W)	Laser ablation diameter	Width of bridge formed
1	Micro-A	18 µm	15.8 µm	1.68 µm
2	Micro-B	17.5 µm	15.8 µm	1.39 µm
3	Micro-C	16.5 µm	15.8 µm	1.23 µm
4	SubMicro-D	16 µm	15.8 µm	732 nm

3.1 AFM analysis of Micro-A

When fabricating the bridge Micro-A, the separation distance between the laser ablation spots (S_W) along the length of the square sample was set at 18 μm. This setting determines the width of the bridge. The separation distance between the laser ablation spots (S_L) along the width of the square sample was set at approximately 5 μm. This setting determines the length of the bridge. The laser ablation diameter using the 30 mm focal length convex lens was 15. 8 μm. As a result, a bridge of width 1.68 μm and length 12.79 μm was achieved as can be seen in figure 2. We focus on a very small scan area on the sample that is $20.5 \times 20.5\ \mu m$.

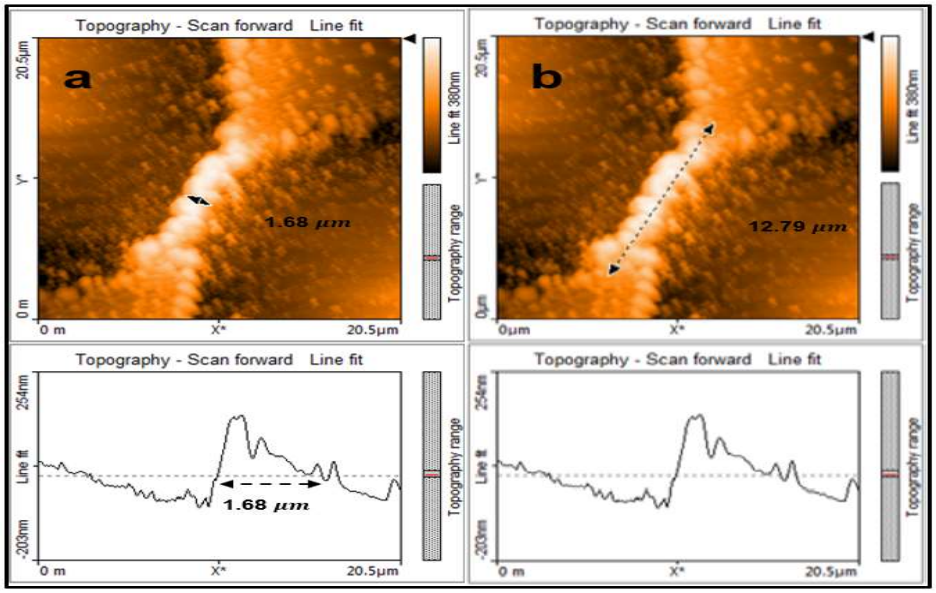

Fig. 2 (a) Topography line fit shows the width of the bridge at 1.68 μm and (b) Topography line fit shows the length of the bridge at 12.79 μm

The measurements are taken using the AFM as the cantilever tip scans transversely at 90 degrees to the laser ablation spot. By using the topography line fit shown in figure 2 (a) the width of the bridge is presented as an amplitude above the zero axis. The width of the amplitude shown in between the black arrows in the figure is 1.68 μm.

3.2 AFM analysis of Micro-B

In the bridge Micro-B, the separation distance between the laser ablation spots (S_W) along the length of the square sample was set at 17.5 μm. The separation distance between the laser ablation spots (S_L) along the width of the sample was set at 5 μm, just as for Micro-A. The laser ablation diameter remained the same as 15.8 μm. A bridge of width 1.39 μm and length 12.26 μm was fabricated as can be seen in figure 3. Again, the scan area was set at $20.5 \times 20.5\ \mu m$. Therefore, by reducing the separation distance between the laser ablation spots (S_W) and keeping the laser ablation diameter constant one can produce a bridge of smaller width as per equation (1).

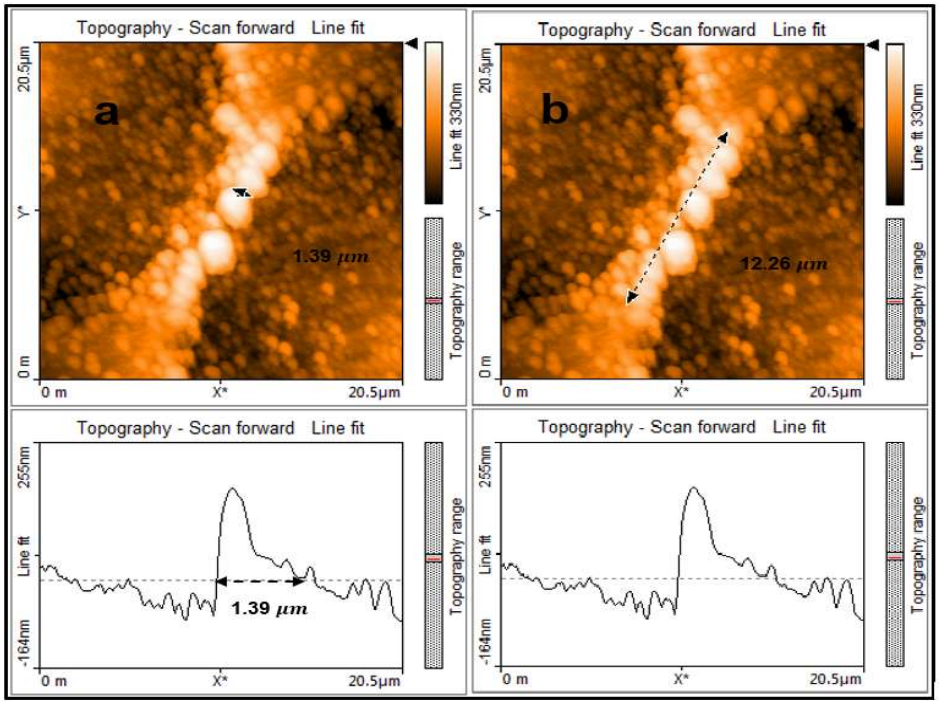

Fig. 3 (a) Topography line fit shows the width of the bridge at 1.39 μm and (b) Topography line fit shows the length of the bridge at 12.26 μm

The measurements were taken with an AFM. In the topography line fit in panel figure 3 (a) the width of the bridge is presented as an amplitude above the zero axis. The width of the amplitude in between the black arrows in the figure is 1.39 μm.

3.3 AFM analysis of Micro-C

In the bridge Micro-C, the separation distance between the laser ablation spots (S_W) along the length of the square sample was set at 16.5 μm. The separation distance between the laser ablation spots (S_L) along the width of the sample was set at 5 μm, just as for Micro-A. The laser ablation diameter remained the same as 15.8 μm. Using the theory of equation (1), a bridge of width 700 nm, is expected however, a bridge of width 1.23 μm is achieved as can be seen in figure 4.

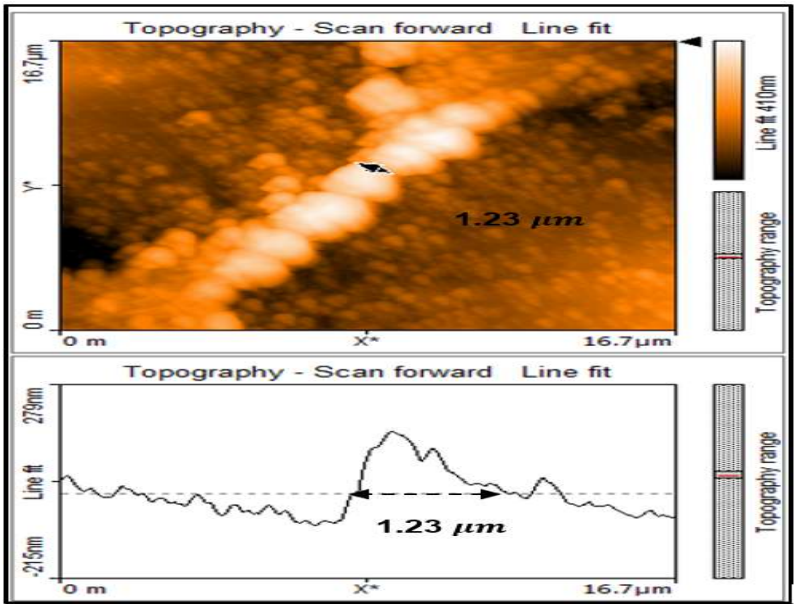

Fig. 4 Topography line fit shows the width of the bridge at 1.23 μm

In order to determine the exact width of this bridge the scan area was reduced to $16.7 \times 16.7\ \mu m$.

3.4 AFM analysis of SubMicro-D

In the design of the bridge SubMicro-D, the separation distance between the laser ablation spots (S_W) along the length of the square sample was set at 16 µm. The separation distance between the laser ablation spots (S_L) along the width of the sample was set at 5 µm, just as for Micro-A. A bridge of width 732 nm was achieved as can be seen in figure 5. The scan area was set at $18.8 \times 18.8\ \mu m$. The figure shows that if we machine any narrower the bridge can collapse. The reason is because we are approaching the diffraction limit of fabricating small structures with the femtosecond laser, which has a wavelength of 775 nm. In addition, in figure 5 it can be seen that there is some thermal degradation on the YBCO thin film. This is shown by the different phases of ablation close to the bridge. There is a dark phase where there is more heating closer to the bridge and a lighter phase where there is less heating away from the bridge in the diameter of the laser ablation spot.

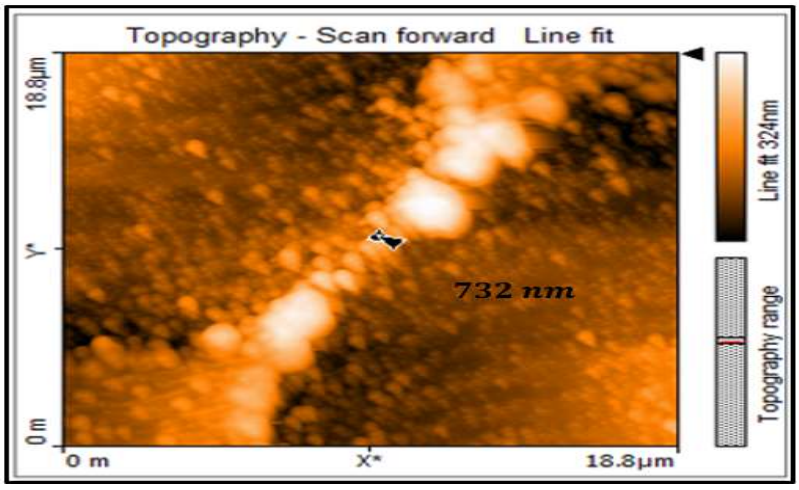

Fig. 5 Topography line fit shows the width of the bridge at 732 nm

4. Conclusion

In conclusion three micron-sized bridges; Micron-A, Micron-B, Micron-C and one sub-micron sized bridge; SubMicron-D were fabricated on superconductive YBCO thin film for possible use as a Josephson junction. These bridges were analyzed for their dimensions with the aid of the AFM. In the end it was discovered that the smaller the separation distance between the laser ablation spots S_W along the length of the square sample, the smaller the width of the bridge that is fabricated. This is the case if the laser ablation diameter is kept constant. There is however a limitation on the smallest width of the bridge that can be fabricated which will depend on the wavelength of the laser.

References

1. Vogel, A.; Noack, J.; Huttman, G. and Paltauf, G. Mechanisms of femtosecond laser nanosurgery of cells and tissues. *Appl.Phys.B* **2005**, 81, 1015-1047.
2. Yao, J. et al. Selective appearance of several laser-induced periodic surface structure patterns on a metal surface using structural colors produced by femtosecond laser pulses. *Appl.Surf.Sci.* **2012**, 258, 7625-7632. Available [Online], https://doi.org/10.1016/j.apsusc.2012.04.105.
3. Wang, S.Y.; Ren, Y.; Cheng, C.W.; Chen, J.K. and Tzou, D.Y. Micromachining of copper by femtosecond laser pulses. *Appl.Surf.Sci.* **2013**, 265, 302-308. Available [Online], https://doi.org/10.1016/j.apsusc.2012.10.200.
4. Bian, Q.; Yu, X.; Zhao, B.; Chang, Z. and Lei, S. Femtosecond laser ablation of indium tin-oxide narrow grooves for thin film solar cells. *Opt.LaserTechnol.* **2013**, 45, 395-401. Available [Online], https://doi.org/10.1016/j.optlastec.2012.06.018.
5. Campbell, T.A.; Haugan, T.J.; Maartense, I.; Murphy, J.; Brunke, L. and Barnes, P.N. Flux pinning effects of Y_2O_3 nanoparticulate dispersions in multilayered YBCO thin films. *Physica C* **2005**, 423, 1-8. Available [Online], https://doi.org/10.1016/j.physc.2004.09.018.
6. Wang, W.T. et al. Chemical solution deposition of YBCO thin film by different polymer additives. *Physica C* **2008**, 468, 1563-1566. Available [Online], https://doi.org/10.1016/j.physc.2008.05.067.
7. Guo, L.S. et al. Liquid phase epitaxy of REBCO (RE=Y, Sm) thick films on YBCO thin film deposited on LAO substrate. *J. Cryst. Growth* **2013**, 366, 47-50. Available [Online], https://doi.org/10.1016/j.jcrysgro.2012.12.019.
8. Jacob, M.V.; Mazierska, J.; Savvides, N.; Ohshima, S. and Oikawa S. Comparison of microwave properties of YBCO films on MgO and $LaAlO_3$. *Physica C* **2002**, 372-376, 474-477. Available [Online], https://doi.org/10.1016/S0921-4534(02)00725-6.
9. Ryu, C.; Blackburn, P.W.; Blinova, A.A. and Boshier, M.G. Experimental Realization of Josephson Junctions for an Atom SQUID. *Phys. Rev. Lett.* **2013**, 111, 205301. Available [Online], https://doi.org/10.1103/PhysRevLett.111.205301
10. Jeanneret, B. and Benz, S.P. Application of the Josephson effect in electrical metrology. *Eur. Phys. J. Special Topics* **2009**, 172, 181-206. Available [Online], https://doi.org/10.1140/epjst/e2009-01050-6.
11. Ren, H. et al. Topological superconductivity in a phase-controlled Josephson junction. *Nature* **2019**, 569, 93-98. Available [Online], https://doi.org/10.1038/s41586-019-1148-9
12. Cassidy, M.C. et al. Demonstration of an ac Josephson junction laser. *Science* **2017**, 355, 939-942. Available [Online], https://doi.org/10.1126/science.aah6640.
13. Dana, S.K.; Sengupta, D.C. and Edoh, K.D. Chaotic Dynamics in Josephson Junction. *IEEE Trans. Circuits Syst. I: Fundamental Theory and Applications* **2001**, 48, 990-996. Available [Online], https://doi.org/10.1126/science.aah6640.
14. Bouchiat, V. Detection of magnetic moments using a nano-SQUID: limits of resolution and sensitivity in near-field SQUID magnetometry. *Supercond. Sci. Technol* **2009**, 22, 064002. Available [Online], https://iopscience.iop.org/article/10.1088/0953-2048/22/6/064002
15. Korte, F. et al. Towards nanostructuring with femtosecond laser pulses. *Appl. Phys. A* **2003**, 77, 229-235. Available [Online], https://doi.org/10.1007/s00339-003-2110-z.
16. Gross, L.; Mohn, F.; Moll, N.; Liljeroth, P. and Meyer, G. The Chemical Structure of a Molecule Resolved by Atomic Force Microscopy. *Science* **2009**, 325, 1110-1114. Available [Online], https://doi.org/10.1126/science.1176210
17. Muller, D.J. and Dufrene, Y.F. Atomic force microscopy: a nanoscopic window on the cell surface. *Trends Cell Biol.* **2011**, 21, 461-469. Available [Online], https://doi.org/10.1016/j.tcb.2011.04.008

18. Li, N. et al. An Atomic Force Microscopy Study of Single-Layer FeSe Superconductor. *Appl. Phys. Express* **2013**, 6, 113101. Available [Online], https://doi.org/10.7567/APEX.6.113101
19. Gonnelli, R. S. Atomic force microscopy in the surface characterization of semiconductors and superconductors. *Philos. Mag. B* **2000**, 80, 599-609. Available [Online], https://doi.org/10.1080/13642810008209768
20. Koblischka, M. R.; Winter, M. and Hartmann, U. Nanostripe structures in $SmBa_2Cu_3O_x$ superconductors. *Supercond. Sci. Technol.* **2007**, 20, 681-686. Available [Online], https://doi.org/10.1088/0953-2048/20/7/016
21. Umenne, P. Fabrication of Nano Josephson Junctions Using the Femtosecond Laser Technique on High T_C Superconducting $YBa_2Cu_3O_7$ thin Films. *PhD Thesis University of South Africa* **2018,** Available [Online], http://hdl.handle.net/10500/23646